Temperature dependence of the resistivity and structure of carbon nanotube films containing various kinds of tubules

O. E. Omel'yanovskiĭ and V. I. Tsebro[1)]
Lebedev Physical Institute, Russian Academy of Sciences, 117924 Moscow, Russia

O. I. Lebedev, A. N. Kiselev, V. I. Bondarenko, N. A. Kiselev
Institute of Crystallography, Russian Academy of Sciences, 117334 Moscow, Russia

Z. Ja. Kosakovskaja
Institute of Radio Engineering and Electronics, Russian Academy of Sciences, 103907 Moscow, Russia

L. A. Chernozatonskiĭ
Institute of Chemical Physics, Russian Academy of Sciences, 117977 Moscow, Russia

(Submitted 9 August 1995)
Pis'ma Zh. Éksp. Teor. Fiz. **62**, No. 6, 483–490 (25 September 1995)

The temperature dependence of the resistivity is measured over a range of 4.2 to 300 K on carbon films containing multilayer nanotubes (MLTs) or single-layer nanotubes (SLTs) oriented perpendicular to the substrate. The structure of these films is examined by high-resolution electron microscopy. At low temperatures, the planar resistivity of all the films is well fit by the expression $\ln \rho \propto [T_0/T]^{1/n}$, with $n=4$ and $T_0 \sim 10^6$ K for the MLT films but with $n=2$ and $T_0 \sim 20$ K for the films containing bundles of SLTs 0.71 nm in diameter. The data obtained are considered in terms of the variable-range hopping conductivity. The estimations made show a fairly high density of states at the Fermi level ($\sim 10^{21}$ $eV^{-1}cm^{-3}$) for the films containing SLTs. © *1995 American Institute of Physics.*

Since the discovery of carbon nanotubes (buckytubes)[1] their electronic properties have been of great interest. Most studies are band-structure calculations for single nanotubes (see, for example, the review in Ref. 2). It follows from these studies that the type of electronic structure is subject to variation from metallic to semiconducting depending on the tubule diameter and the degree of helical arrangement. There have been experimental studies devoted to the longitudinal conductivity of nanotube bundles.[3,4] In Ref. 3 the conductivity of a big multiple bundle several tens of microns in diameter was investigated, and the resistance of a single carbon nanotube bundle ~50 nm in diameter has been successfully measured using "state-of-the-art" technique by R. Langer and co-workers.[4] In general terms, both studies showed a semimetallic conductivity of the buckytubes, with weak localization behavior at low temperatures.

A variety of techniques have been used to demonstrate the possibility of producing buckytube films by electron-beam evaporation of graphite.[5–9] Among them scanning tunneling microscopy (STM) has been the most often used.[5,6,8,9] In particular, STM has

TABLE I.

sample	substrate	t_f,nm	D,nm	n_l	ρ(250K/25K/5K)	n	T_0,K	T^*,K
#1	glass	150	0.72	1 [a]	0.014/0.039/0.11	2	16	15
#2	glass	170	0.72	1 [a]	0.0086/0.023/0.074	2	23	25
#3	(111)Si	93	$\leq$25	11–34	0.26/180/250000 [c]	4	$1.1 \cdot 10^6$	165
#4	glass	120	0.72	1 [b]	0.0052/0.011/0.019	4	39	48

[a] bundles of STL's; [b] separate SLT's; [c] obtained by extrapolation.

revealed that the surface relief of films obtained at medium carbon flux densities is made up of dome-shaped and/or conical tips. In films obtained under slightly different conditions, STM showed a surface relief consisting of rods 1 nm in diameter.[6] High-resolution electron-microscope (HREM) imaging was used to examine films deposited on different substrates at medium carbon flux densities.[7] Most of them did consist of multilayer nanotubes (MLTs). Scanning-electron-microscope (SEM) imaging of broken films revealed a fiber structure oriented toward the carbon flow.[6,8] Such a structure is most probably formed by the aggregates of MLTs or by bundles of single-layer nanotubes (SLTs). The bundles of SLTs were first observed by N. Kiselev and others[10] in those films where STM revealed 1 nm rods. As was mentioned in Ref. 11, the kind of buckytube structure is influenced not only by the carbon flux density but also by the type of substrate and its temperature as well as by the vacuum conditions and the arrangement of the deposition process.

The purpose of this paper is to report an experimental study of the structure and of the temperature dependence of the resistivity of similarly constituted buckytube films prepared under different conditions and, hence, having considerably different structures. Buckytube films were deposited on (111)Si and glass substrates using an electron-beam deposition technique described elsewhere.[5,6] During the deposition process, the carbon flow was directed normally to the substrate. Hence the orientation of the nanotubes is expected to be normal to the plane of the substrate. For all the investigated films the type of substrate and film thickness (t_f) are given in Table I. For sample #4 the deposition process was interrupted, and a considerable difference in its properties is seen in the data.

The specimens for HREM were prepared by scraping the film off the substrate. Detached fragments were subjected to ultrasonic treatment in acetone. The images were taken in a Philips EM 430ST instrument operated at 200 kV. Computer simulation based on the multislice method[12] was used for image interpretation.

According to the HREM examination of the film deposited on (111)Si (sample #3), the main component of the film consists of MLTs like those observed by Iijima.[1] The number of layers in these MLTs ranges from 11 to 32. The length of the tubules is comparable to the film thickness. In many cases, HREM imaging demonstrates the outer layers of nanotubules being destroyed. In some instances one can observe an external amorphous layer. An example of the MLTs from this spectrum is shown in Fig. 1a.

Another type of structure (Fig. 1b) was observed in the films deposited on the glass substrate under those conditions for which STM revealed a rod relief (samples #1 and #2).[5,6] This type can be characterized as a buckytube bundle with a longitudinal striation having a periodicity of 1.06 nm. The maximum length of the bundles is also comparable

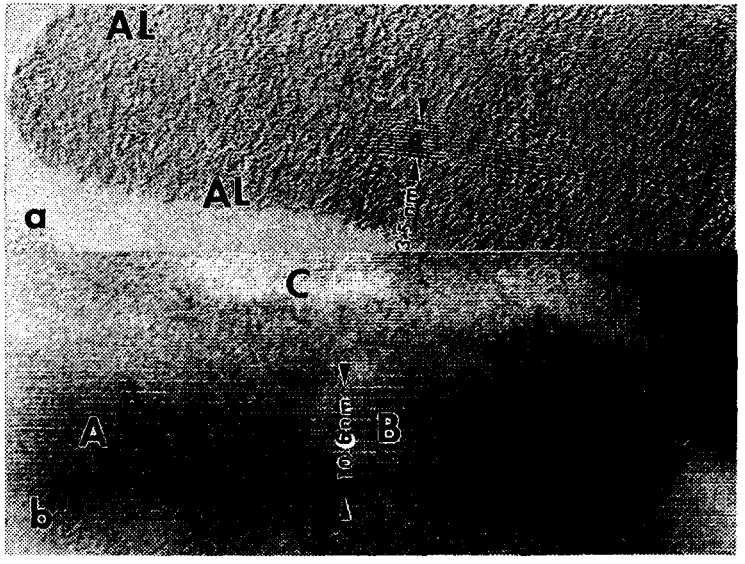

FIG. 1. HREM images of carbon nanotube films: (a): a MLT covered by an amorphous layer (AL) from the film on the (111)Si substrate; (b): a bundle of SLTs from the film on the glass substrate. Marked by A, B, and C are regions of different contrast.

to the film thickness. In addition to this major periodicity, HREM imaging revealed a finer structure which is expressed as additional longitudinal bands of various contrast. In some images an "oblique" periodicity running at an angle to the bundle axis was observed.

The following assumptions, subsequently tested by computer simulation, were made: (1) the observed bundles are formed by 100–1000 SLTs (see also Ref. 10): (2) these nanotubes do not have any intermediate layers and form close, probably hexagonal, packing; (3) adjacent nanotubes are shifted with respect to one another in a certain order, i.e., the bundle can be regarded as a quasicrystal.

For image simulation, one of the possible packings of hexagons, the so-called "zigzag" packing, and a chiral angle $\theta=0$ were used.[2,13] Such a zigzag tubule, having a tubular diameter of 0.71 nm, is formed of rings of 9 hexagons each. The choice of parameters for the simulation is dictated by the observed periodicity (1.06 nm) and the distance between carbon layers or, more properly, the walls of the tubules (0.35 nm).

The image simulation has been fulfilled for two different mutual orientations of the close-packed tubes. In the first version, the packing is assumed to be a simple translation of the tubes. In this case, a certain similarity with the experimental images has been obtained, but the oblique periodicity cannot be explained. In the second version, one of the tubes in the unit cell is rotated by 20°, and the other one is shifted along the axis. Just then, the oblique periodicity is observed at a certain defocus Δf and specimen thickness

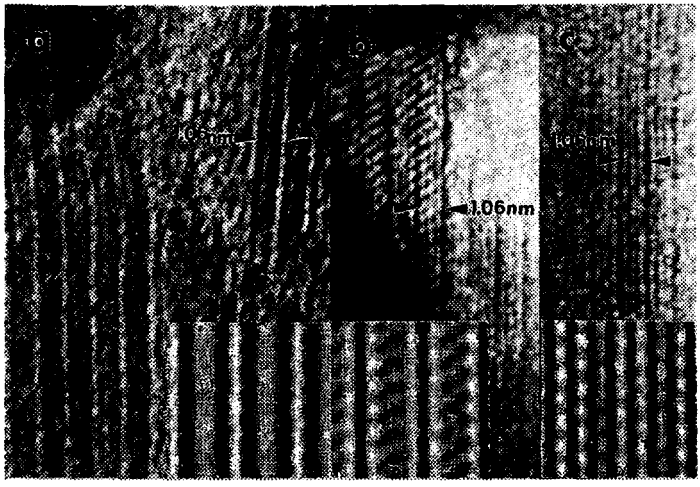

FIG. 2. HREM images of the different kinds of SLT bundles. Shown at the bottom are simulated images along [110]: (a): $t=2.4$ nm, $\Delta f=-20$ nm; (b): $t=1.3$ nm, $\Delta f-10$ nm; (c): $t=0.8$ nm, $\Delta f=-10$ nm (see designations in text).

t. Various kinds of HREM images as well as the selected image simulations are presented in Fig. 2.

From analysis of the image simulations one can conclude that the above structure model is consistent with the experimental data, i.e., the observed structure can be really considered as the bundles of hexagonally packed zigzag nanotubes 0.71 nm in diameter and with chiral vector (9,0).

In the micrographs, the SLT bundles are set off with a pronounced contrast, so that their images must result from the superposition of a few nanotubes. On the other hand, the computer simulation images resembling the experimental images with oblique periodicity correspond only to small thicknesses (0.8–1.3 nm). This contradiction could be explained by assuming that the bundles are tilted by 5–15° to the electron beam. In this case, a preliminary image simulation shows that the oblique periodicity is revealed at greater thicknesses.

The hexagonal packing and cylindrical shape of the nanotubes is not the only possible tentative design of the bundles. A rectangular packing of tubules having hexagonal cross section has been also considered. In this case, the contrast of the tube walls in the simulated images is increased as well as the visibility of the inner oblique structure.

The above interpretation of the experimental images as bundles of SLTs seems to be the best one. Nevertheless, a striated structure containing moire fringes could be also obtained within the fibrillar model, in which the bundle is formed by carbon ribbons, or within the lamellar model, where these fringes originate from a bent carbon layer.[14] However, in both cases the expected striation periodicity is much larger than in our experimental micrographs. Besides, it appears that neither of these models can explain the STM data.[5,6,8,9] It seems that the final judgment about the type of observed structure

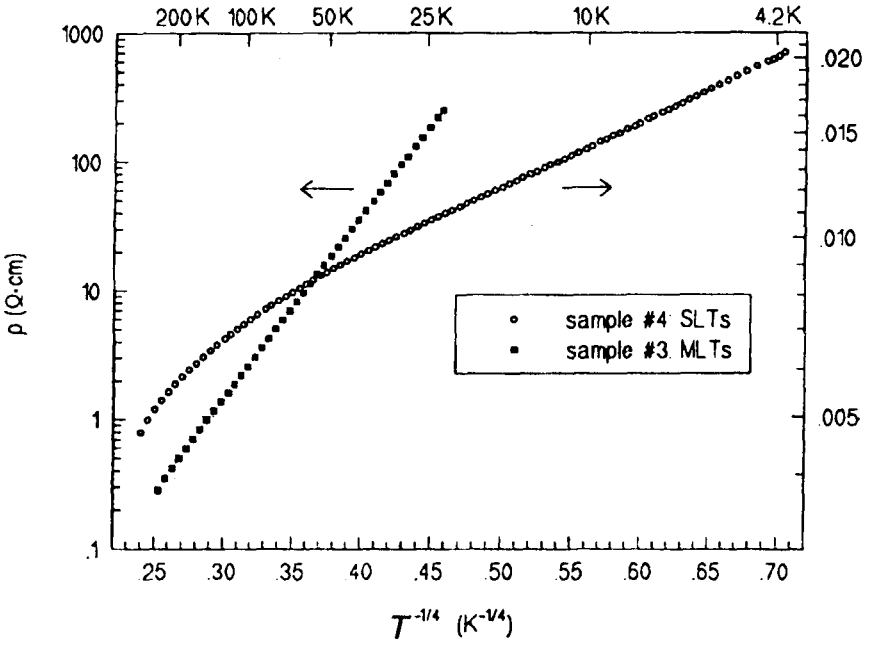

FIG. 3. Logarithmic resistivity versus $T^{-1/4}$ for the film with MLTs (left scale) and for the film with separate SLTs (right scale).

could be made after the analysis of electron diffraction patterns and plan-view HREM investigations of the films.

It should be noted that the nanotubes comprising the bundles are sensitive to radiation damage. The effect of an electron beam on relatively small bundles and separate tubules is more pronounced. Along with SLTs a small amount of fullerite C_{60} crystals was revealed. In sample #4 mentioned above (corrupted deposition process), the bundles of nanotubes were not observed but, instead, a small quantity of SLTs of approximately 0.71 nm in diameter appeared. They were surrounded by a structureless, perhaps amorphous material. As will be shown below, the temperature dependence of the resistivity of this film is fundamentally different from that of the films containing nanotube bundles.

Measurements of the resistivity ρ (over the temperature range from 4.2 to 300 K) were carried out on the same samples whose structure was concurrently investigated by HREM. The standard dc four-probe method was used. The electrical contacts with the films measured $\sim 2 \times 12$ mm and were made of silver epoxy. It is apparent that, having the nanotube axes normal to the substrate or slightly tilted to it, the film passed the current across the tube axes.

It turned out that at temperatures below a certain value (T^*) all the films exhibit precisely the temperature-dependent resistivity $\rho(T)$ of the form

$$\rho(T) = \rho_0 \exp[(T_0/T)^{1/n}] \tag{1}$$

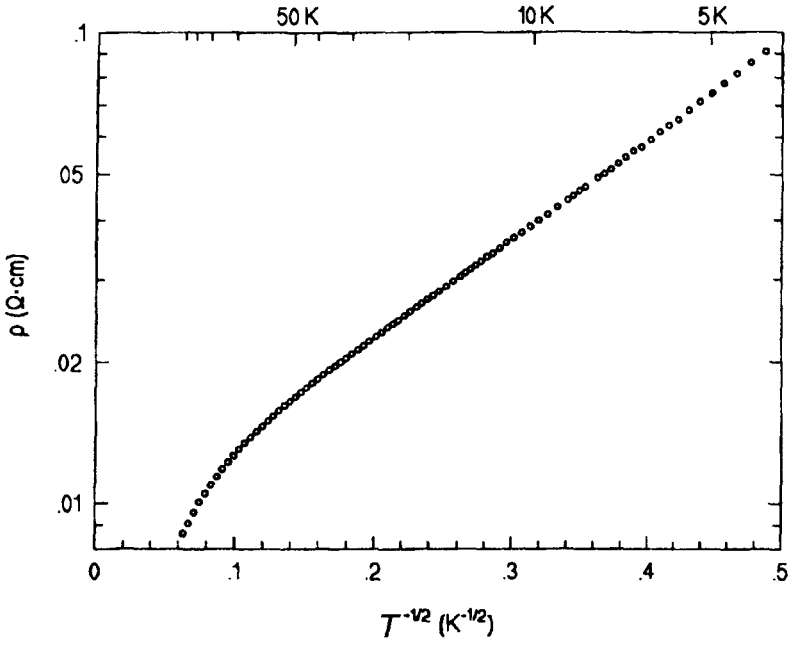

FIG. 4. Logarithmic resistivity versus $T^{-1/2}$ for the film with the bundles of SLTs.

typical of the variable-range hopping (VRH) mechanism. However, the different types of films exhibited radically different $\rho(T)$ behavior in respect to the values of n and T_0 in Eq. (1).

Thus the films containing multilayered nanotubes are characterized by rather high values of the resistivity at low temperature, the many-decade temperature dependence of which is a characteristic of a strongly localized system. At $T<150-200$ K, the $\rho(T)$ dependence of these films strictly follows Eq. (1) with $n=4$. The value of T_0 exceeds 10^6 K. As an example, the logarithmic resistivity versus $T^{-1/4}$ for sample #3 is shown in Fig. 3 (left scale).

On the other hand, the films containing the bundles of SLTs have significantly lower resistivity, and their $\rho(T)$ dependence at temperatures below 15–25 K strictly follows Eq. (1) with $n=2$. In Fig. 4, the logarithmic resistivity versus $T^{-1/2}$ is plotted for sample #2.

In Table I the main structure parameters of the nanotubes comprising the films, namely, the outer nanotube cage diameter D and the number of carbon layers n_l, as well as the parameters of the temperature-dependent resistivity: the measured values of ρ (in units of $\Omega\cdot$cm) at temperatures of 5, 25 and 250 K, and the values of n and T_0 in Eq. (1), are summarized for the main types of nanotube films investigated. Also presented is the temperature T^* above which the experimental $\rho(T)$ dependence notably deviates from Eq. (1).

Attention is drawn to the properties of sample #4. At room temperature, the resistivity of this film, containing separate SLTs surrounded by a structureless material, is

even below that of the films with the bundles of SLTs but its resistivity $\rho(T)$ at $T<50$ K follows Eq. (1) with $n=4$ rather than with $n=2$ (see Fig. 3, right scale). The value of T_0 is accordingly far lower than those observed in the films containing MLTs.

Thus the $\rho(T)$ dependence with $n=4$, which is typical of the 3D Mott conductivity, holds for the films containing either MLTs or separate SLTs surrounded by a structureless material.

From the well-known formula[15] for T_0

$$T_0=\frac{21.2}{k_B N(E_F)\xi^3}, \tag{2}$$

it follows that at density of states at the Fermi level $N(E_F)\sim 10^{18}$ $\mathrm{eV}^{-1}\mathrm{cm}^{-3}$ (in accordance with the data for amorphous carbon[16]), the estimated localization length $\xi\sim 6$ nm for the films with MLTs ($T_0\sim 10^6$ K). This is consistent in order of magnitude with the mean radius of the nanotubes. As for the other type of film for which $n=4$ in Eq. (1), it is apparent that the very small value of $T_0\sim 40$ K for sample #4 with separate SLTs implies a vastly greater value of $N(E_F)\sim 6\cdot 10^{21}$ $\mathrm{eV}^{-1}\mathrm{cm}^{-3}$ at $\xi\sim 10$ nm.

It should be noted that the high temperature values of ρ of the films with MLTs are comparable with those of as-prepared activated carbon fibers (ACF).[17] ACFs are a unique class of porous materials consisting almost exclusively of nanopores with an average size of 1 nm. However, the $\rho(T)$ dependence for as-prepared ACFs follows Eq. (1) with $n=2$ and $T_0\sim 500$ K (Ref. 17). After heat treatment at ~ 1000 K, a collapse of nanopores occurs that results in a considerable decrease in ρ and T_0. The temperature dependence $\rho(T)$ of these heat-treated ACFs is similar to that of our films containing the bundles of SLTs, the only difference being that, in our instance, the absolute values of ρ and T_0 are less by an order of magnitude. Besides that, deviations from linearity of the logarithmic resistivity versus $T^{-1/2}$ begin at much lower temperature.

The resistivity of granular metals (see, for example, Ref. 18) and of VRH systems with a developed Coulomb gap in the density of states near the Fermi level[19] is known to follow Eq. (1) with $n=2$. In the latter case, the equation for T_0 is given by

$$T_0=\frac{\beta e^2}{k_B \kappa \xi}, \tag{3}$$

where e is the electronic charge, κ the dielectric constant, and β a dimensionless factor of the order of unity. If we take $T_0\sim 20$ K (as determined by our measurements) and $\kappa\sim 100$ (as has been estimated[17] for heat-treated ACF), then $\xi\sim 8$ nm, which is again compatible with the radius of the SLT bundle.

Since $N(E_F)$ has not been directly included in Eq. (3), it can be estimated with the use of the experimental T^* value, which can be determined with some degree of certainty as the temperature where deviation from the linearity of $\ln\rho$ versus $T^{-1/2}$ begins. For this purpose, it is necessary to equate the energy interval near the Fermi level

$$\epsilon_0(T)=\frac{(k_B T)^{3/4}}{[N(E_F)\xi^3]^{1/4}} \tag{4}$$

in which the states involve hopping, to the value of the Coulomb gap

$$\Delta = \frac{e^3 N(E_F)^{1/2}}{\kappa^{3/2}} \tag{5}$$

(see, for example, Ref. 15). From the equation $\epsilon_0(T^*)=\Delta$ it follows that $N(E_F)\sim 5\cdot 10^{20}$ eV^{-1} cm^{-3} for $T^*\sim 10$ K and the κ and ξ values mentioned above.

In turn, the carrier density $n_c = 2N(E_F)\epsilon_0(T)$, which according to Eq. (4) is proportional to $T^{3/4}$ at low temperatures, can be estimated at $T\sim 25$ K as $n_c\sim 3\cdot 10^{16}$ cm^{-3} for the films with MLTs, $n_c\sim 1.4\cdot 10^{19}$ cm^{-3} for the films with separate SLTs, and $n_c\sim 2.5\cdot 10^{18}$ cm^{-3} for the films with the bundles of SLTs.

In summary, it may be said that these simple estimates show that the films containing SLTs (separate or assembled into bundles) and exhibiting variable-range hopping conductivity are, in such a situation, systems with a fairly high ($\sim 10^{21}$ $\mathrm{eV}^{-1}\mathrm{cm}^{-3}$) density of states at the Fermi level. Packing of the tubes into ordered assemblies, which are oriented perpendicular to the substrate, is probably of key importance because it leads to a change of the law governing VRH conductivity at low temperatures from $T^{-1/4}$ to $T^{-1/2}$. This can be interpreted as the appearance of a Coulomb gap in the density of states, which in turn can be a consequence of the assembling of the nanotubes into bundles. The absence of amorphous substance between the tubules in the bundle and its fairly high homogeneity and ordered arrangement make it possible to refer to such a bundle as a quasicrystal. It is also possible that these ordered nanotube bundles play the role of metal granules, with tunneling between nearest neighbors. In this case the conductivity also follows the law $-\ln\sigma \propto T^{-1/2}$ (Ref. 18). Which of these descriptions is more appropriate will be seen from further studies of the properties of carbon nanotube films. Among those properties, the electrical transport in magnetic fields should be studied first.

This material is based upon work supported by the Intersectoral Scientific and Technological Program of Russia "Fullerenes and Atomic Clusters" under Grant 4 as well as by the International Scientific and Technological Center under Grant 079. The authors acknowledge useful discussion with A. S. Kotosonov.

[1)]e-mail: tsebro@sci.lpi.ac.ru

[1]S. Iijima, Nature **354**, 56 (1991).
[2]M. S. Dresselhaus, G. Dresselhaus, and P. C. Eklund, J. Mater. Res. **8**, 2054 (1993).
[3]S. N. Song, X. K. Wang, R. P. H. Chang, and J. B. Ketterson, Phys. Rev. Lett. **72**, 697 (1993).
[4]L. Langer, L. Stockman, J. P. Heremans *et al.*, J. Mater. Res. **9**, 927 (1994).
[5]Z. Ja. Kosakovskaja, L. A. Chernozatonskii, and E. A. Fedorov, JETP Lett. **56**, 26 (1992).
[6]L. A. Chernozatonskii, E. A. Fedorov, Z. Ja. Kozakovskaja *et al.*, JEPT Lett. **57**, 35 (1993).
[7]L. A. Chernozatonskii, Z. Ja. Kosakavskaja, A. N. Kiselev, and N. A. Kiselev, Chem. Phys. Lett. **228**, 94 (1994).
[8]L. A. Chernozatonskii, Z. Ja. Kosakovskaja, E. A. Fedorov, and V. I. Panov, Phys. Lett. A **197**, 40 (1995).
[9]L. A. Chernozatonskii, Yu. V. Gulyaev, Z. Ja. Kosakovskaja *et al.*, Chem. Phys. Lett. **233**, 63 (1995).
[10]N. A. Kiselev, L. A. Chernozatoskii, Z. Ja. Kosakovskaja *et al.*, *Ninth International Conference on Microscopy of Semiconducting Materials, 20–23 March 1995*, University of Oxford, Oxford (1995).
[11]Z. Ja. Kosakovskaja, *Abstracts to 1994 Fall Meeting of Materials Research Society, page 260.*
[12]J. M. Cowley, *Diffraction Physics* second revised edition, (North-Holland, Amsterdam) (1990).
[13]L. A. Chernozatonskii, Phys. Lett. A **166**, 55 (1992).
[14]A. Oberlin, Carbon **17**, 7 (1979).

[15] B. I. Shklovskii and A. L. Efros, *Electronic Properties of Doped Semiconductors* (Volume 45 of Springer Series in Solid State Sciences), Springer, Verlag, Berlin (1984).
[16] J. J. Hauser, Solid State Comm. **17**, 1557 (1975).
[17] A. W. P. Fung, Z. H. Wang, M. S. Dresselhaus *et al.*, Phys. Rev. B **49**, 17325 (1994).
[18] P. Sheng, Philos. Mag., **65**, 357 (1992).
[19] A. L. Efros and B. I. Shklovskii, J. Phys. C (Solid State Phys.) **8**, L49 (1975).

Published in English in the original Russian journal. Edited by Steve Torstveit.